ON-LINE LOCATION OF PARTIAL DISCHARGES IN AN ELECTRICAL ACCESSORY OF AN UNDERGROUND POWER DISTRIBUTION NETWORK

François LÉONARD, Hydro-Québec, IREQ, (Canada), leonard.francois@ireq.ca
Daniel FOURNIER, Hydro-Québec, V-P Distribution, (Canada), fournier.daniel.3@hydro.qc.ca
Bruno CANTIN, Hydro-Québec, IREQ, (Canada), cantin.bruno@ireq.ca

ABSTRACT

Many of the power failures occurring at cable joints in Hydro-Québec's underground distribution network are due to partial discharges inside the joints. The network consists mainly of XLPE cable with rubber-moulded accessories. After five years of R&D, a new on-line detection device for locating partial discharges (PD) in the harsh radiofrequency environment of a city is about to be deployed. We have modified a known design by adding an electrostatic shield, an embedded filter and a variable-gain amplifier. Two sensors are clamped around the helical-strand shield of the cable on each side of the electrical accessory. A third sensor, clamped on the semiconductor shield, is used to confirm the presence of high voltage and to measure the line phase angle. Hundreds of underground measurements downtown and in the suburbs demonstrate the diagnostic accuracy. This paper presents the new detection concept, the applied signal processing and some of the field results.

KEYWORDS

Partial discharge, XPLE cable, underground distribution network, time domain reflectometry, spectrogram, line phase sensor.

INTRODUCTION

Hydro-Québec began to deploy mobile infrared (IR) thermography units on its underground system at the end of the 1980s. IR thermography is used to locate resistive contacts and dielectric hotspots on-line in the network. Nevertheless, some of these hotspots remain hidden from view and cannot be detected by thermography. To combine good preventive maintenance with guaranteed safety for its workers, in 1993 the Québec power utility therefore started to use a commercial device for the on-line detection of electromagnetic (EM) radiation associated with partial discharges (PDs) present in the network. The EM emission from PDs is therefore measured after the thermography. Inspired by patent No. CA 2013552 [1], this device performs a double-conversion AM (superheterodyne detection) in a narrow band of several kilohertz on a 6.9-MHz carrier. The EM activity in this narrow-band is displayed on a decibel scale. The device has a number of drawbacks however:

1) It does not have the required sensitivity to be able to detect sites with a low rate of discharges.

2) It does not differentiate between a wideband (>100 MHz) very short discharge with a high amplitude and a time-dispersed transient signal with a lower frequency and smaller amplitude.

3) Attenuating an EM wave propagating in the cable to 6.9 MHz is not enough to eliminate signals coming from other manholes.

4) The EMI causes faulty detection. Sometimes, operators can hear music or conversations from the device's loudspeaker.

5) The detection principle is based on the use of a floating capacitive coupling, not ground-referenced, so that the instrument's response appears sensitive to the way it is maintained.

Points 2) and 3) imply that a discharge in adjacent equipment gives a diagnosis indicating the presence of PDs, even if they are located several hundreds of meters from the source [2].

With no ready access to many of its underground installations, Hydro-Québec launched a research program earlier this century in an aim to develop a reliable device for detecting, locating and characterizing discharge sites on-line. There are now some 30 units of a second generation of this new device in operation in the Québec underground network. The PD analyzer (PDA), as it is known, is based on time-domain reflectometry (TDR) and calls for three sensors to be installed on the accessory or the portion of cable to be instrumented; these sensors are connected by a 13-m cable to the device, which is installed outside the manhole. Although the PDA is more complicated to use than the earlier commercial device, we have not found any error in its diagnostics, after more than 1000 field measurements.

HARDWARE DESCRIPTION

After multiple tests in the laboratory and on the underground network, we chose the magnetic sensor proposed by E. F. Steennis at KEMA [3,4]. This sensor comprises a single conducting loop which responds to the longitudinal magnetic field generated by the helical-stranded shield of the cable. However, as this sensor is not very practical to install and responds to noise in a wide band, we made a few improvements (see Fig. 1), namely:

- Addition of a hinge with a connection on the opposite side so as to convert the sensor into a clamp and therefore easy to position.
- Electronics (including a filter and a commutable gain amplifier) built into the sensor.
- Electrostatic shield enveloping the sensor and its electronics.

Since the PD signals observed with this sensor have a bandwidth exceeding 350 MHz, the sensor is attached to a 1

Gs/s digitizer. As illustrated in Figure 2, the signal passes through one protection module and three filter modules. The first is a 1.7-MHz high-pass filter which eliminates AM radio signals, among others. The second is an anti-aliasing filter while the third is one selected from a bank of switchable filters. For example, in the presence of signal saturation by a nearby transmitter station, a low-pass filter is installed to eliminate the signal from the station.

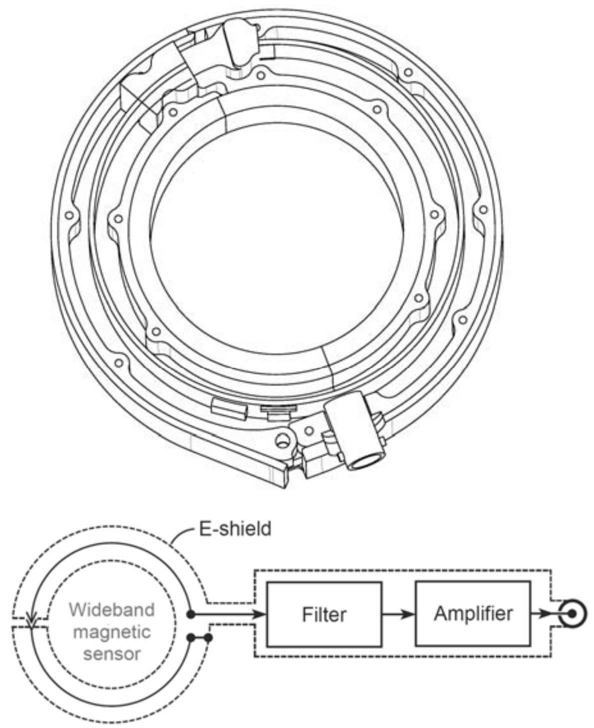

Figure 1: Wideband magnetic sensor, 3D view (top) and schematic (bottom)

The signal is digitized on-line and stored in a circular buffer. At a digitization rate of 1 Gs/s, only those portions of the signals where PDs appear can be stored. The trigger module transmits digitized data from the circular buffer when the amplitude exceeds the triggering amplitude. As the data is cumulated in a rapid-access memory of reduced capacity, this limits the number of trigger events so they can be stored successively.

In the PDA as well as in competitive PD measuring systems, the network phase is measured in order to determine the value of the phase corresponding to each PD. In the proposed system illustrated in Figure 2, the phase information is processed in order to activate or deactivate the trigger mechanism. Here, a line phase sensor is clamped on to the semiconductor covering the cable or joint. The signal that is picked up, in phase with the line voltage, feeds a phase lock loop connected to the trigger controller. This approach offers several advantages including that of forcing an unbiased statistical sampling of the PDs as a function of the phase. For example, when the density of events fills up the RAM in less than one cycle, the triggering mechanism can be reactivated one or more cycles later at the last recorded phase value (Fig. 3). Furthermore, for an active discharge site in a specific range of phases, when the PDs picked up for this site are mostly drowned out by the noise, it is preferable to target this portion of the phase in order to cumulate more PDs and compensate for the noise.

DIGITAL PROCESSING TOOLS

Digital processing is subdivided into five modules: (1) a VHF interference level estimator, (2) a bank of digital filters, (3) a correlator, (4) an external radiation estimator (5) the form factor calculation module.

1- In the presence of a high level of VHS interference compromising the measurement, the first of these modules informs the conditioning unit to that effect and the conditioning unit adds the most appropriate analog filter (see filter bank, Fig. 2) to attenuate the observed noise.

2- The digital filters available are the low-pass, high-pass, pass band, multiple-notch or specialized type, auto-notch, auto-adaptive, FM, TV VHF and TV UHF

3- After juxtaposing the signals from the wide-band sensors, the correlation module gives the main correlation maximums. A possible solution corresponding to each maximum exists to explain the measurement. Each solution is also associated with a correlation coefficient, a channel-to-channel delay and a polarity status (identical or inverse). The module eliminates solutions with a time delay exceeding the propagation time between the two sensors. The statistical distribution of the stored solutions allows us to quantify the likelihood of the most probable solution, i.e. the one retained for making the diagnostic. A low level of likelihood denotes the possibility of a second diagnostic, in which case it is the operator who, sometimes with the help of additional measurements, decides the outcome.

4- Occasional electromagnetic radiation will be observed on the outer surface of the cable which, like a PD located between two sensors, correlates well between these sensors and has a plausible time delay value. The radiation estimation module calculates the number of oscillation half-cycles on the transient of each channel in order to determine the presence of external radiation. Usually a PD has only 3 to 6 half-cycles whereas external radiation has far more oscillations.

5- The PDs are characterized by a short transient and a large spectral spreading, among others. When a PD is observed on a time-frequency distribution such as a spectrogram, the corresponding spot presents a narrow time spread over a broadband frequency. The last module computes the spectrogram of the PD, applies a frequency-time filter (FTF) and computes the ratio of the width of the frequency marginal to the width of the time marginal, a ratio known as the form factor. The form factor increases with the proximity of the PD. External radiation, EMI induced by the cable as well as remote discharges usually have low form-factor values. The time-frequency filter is essential for eliminating the continuous spectral components and background noise in the time-frequency plane.

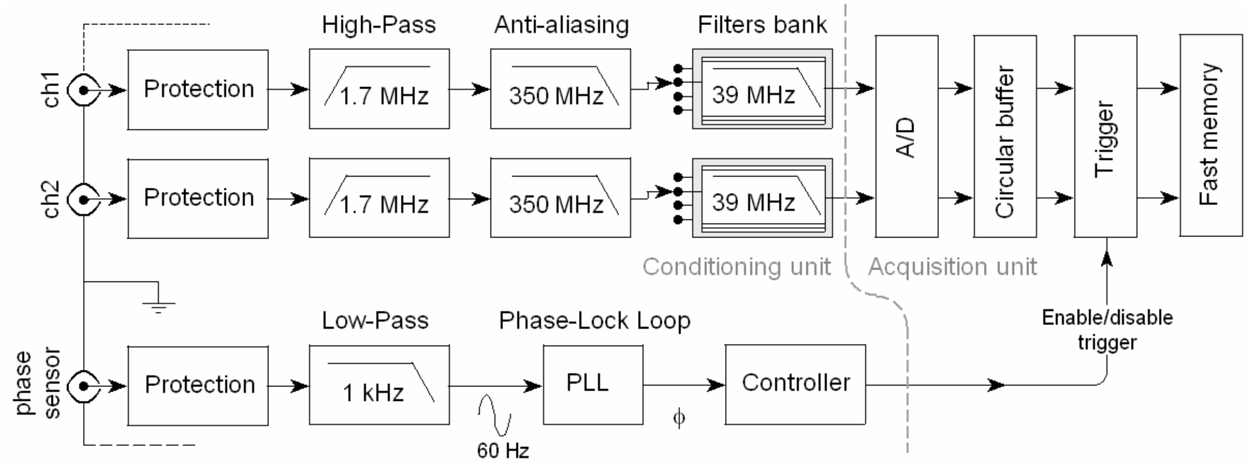

Figure 2: Signal conditioning and acquisition unit.

Results of modules 3, 4 and 5 are transmitted to the diagnostic module. The latter in fact is simply a series of comparators with pre-established thresholds for the minimum correlation levels and form factor. The final diagnostic (absence or presence of PDs) is presented with the values calculated by the different modules: the time curves corresponding to the two channels, the phase value of the line voltage and, in particular, the diagnostic error probability and the presence of a second probable diagnostic. In the case of the latter, the operator may call for a digital filter to be added in order to highlight the right diagnostic. This filter will be applied by module 2 described above.

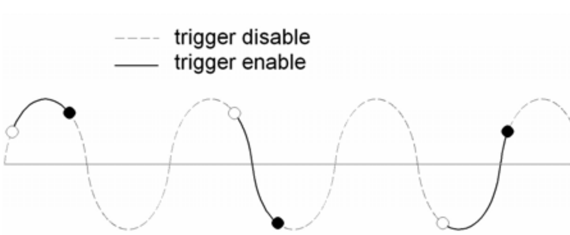

Figure 3: Example of trigger activities controlled by the line phase in order to obtain an unbiased picture of PD phase distribution.

MEASUREMENT PROTOCOL ADOPTED FOR THE UNDERGROUND NETWORK

Before going down into an underground vault, a technician has to make sure the work zone is safe. If necessary, the crew does a scan of the installations by thermography using a robotized camera [5]. If the vault is not shown to have any observable risk, the task of measuring the PDs on the accessories can begin.

To test a cable joint, the crew has placed wideband sensors on each side, as illustrated in Fig. 4a. As soon as the PDA is switched on, it performs a number of self-validation tests. Measuring begins at full-scale amplitude. The gain is gradually increased in order to scan the signal over a smaller and smaller amplitude scale. Measurement stops at the smallest amplitude range or when the number of events picked up per cycle is too high. In this way, we are sure that everything has been done to collect the low-amplitude discharges drowned in a higher-amplitude signal. The TDR of a discharge at the joint displays an inversion of the polarity between the two sensors.

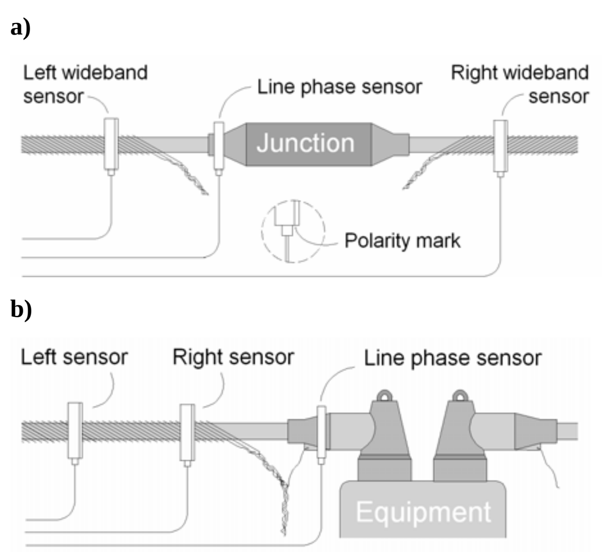

Figure 4: Examples of measuring apparatus on a cable joint (a) and on a unit of equipment (b).

To detect the presence of PDs on the equipment (e.g. a transformer), we have to simply install sensors such as those illustrated in Fig. 4b successively for each connection to the equipment. When all the measurements at the connectors indicate the presence of PDs in the direction of the equipment it means that the PD comes from the latter or from the elbow connected to it. To save time, we can also apply configuration 4a, although the distortion of the wave from one terminal to the other of the equipment reduces the signal coherence between the two sensors so the result is less reliable. If we have any difficulty diagnosing the discharges in a joint because of reflections or other disturbances that reduce the signal coherence between the two sensors, we can apply method 4b to each side of the joint. These methods also allow us to detect faults over distances in excess of 100 m beyond the vault.

CASE STUDIES

Figure 5 presents a TDR example of a discharge observed in a heat-shrinkable splice with a digital notch filter. Inversion of the polarity is noted between the two channels and a rise time of less than 7 ns. The discharge is nearer the left side because the signal appears earlier on this side and has a higher amplitude. It is important to remember that the magnetic sensor yields the derivative of the transient corresponding to the PD.

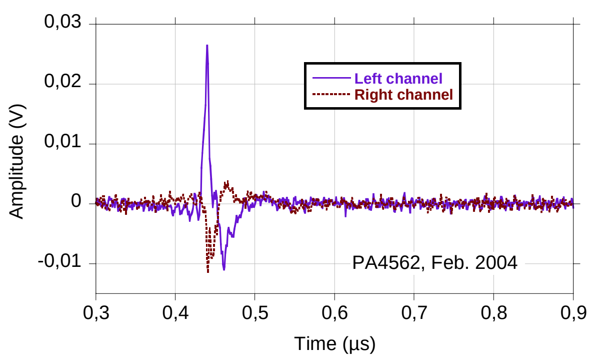

Figure 5: Discharge in a joint recorded on 19-02-2004 in the PA4562. A digital notch filter is applied.

In the presence of a reflection, the echo from the discharge always appears like a smaller PD following the initial PD with a constant time delay. However, the presence of two and occasionally three PDs in rapid succession are sometimes observed, as seen in Fig. 6, and do not come from reflections. Here, the density of the probability of a PD appearing is a function of the time of appearance of the last PD. One plausible explanation would be the close presence of cavities where the discharge in one increases the probability of discharge in the other. The case of two cavities is dealt with on the basis of temperature differences [6]. Any theoretical and/or experimental explanation put forward for this type of measurement would allow us to use our observations of this phenomenon for diagnostic purposes

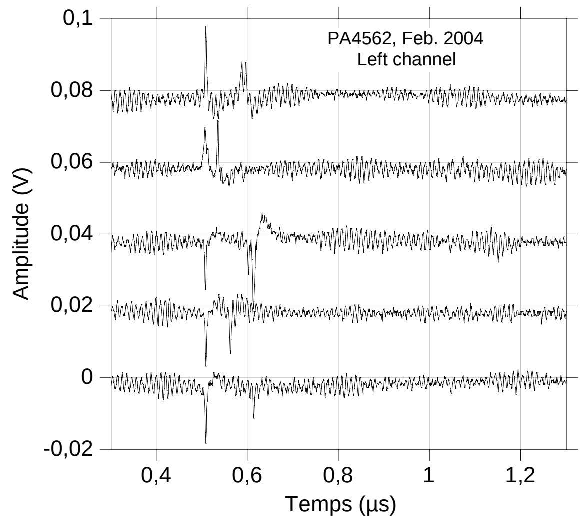

Figure 6: Examples of closely located discharges taken shortly after that illustrated in Fig. 5. A multiple of a 20-mV step was added to separate the curves. No filter was used.

Figure 7 presents a case of huge discharges occurring in a base-mounted transformer installed above ground (TSS1691) and propagating over a distance into several manholes. Note the changes in the amplitude and the time dispersion of the PDs with distance. The transfer function between a PD and the point where it is measured is a function of many details that escape the observer in the field. Moreover, the measured signal corresponds to the derivative of the current pulse propagating on the concentric neutral. It is therefore difficult to make the link between the observed signal and the apparent charge affected by the discharge: the PDs are consequently displayed in volts and not in pC. If necessary, the operator can display the integrated signal but in fact maximum sensitivity is reached when there is no integration and the discharge occurs with a short rise time. For example, a sensitivity of around 1 pC is reached for a PD with a rise time of less than 2 ns. This sensitivity is accessible in the field provided transient noises, often higher in amplitude than the PD signal, are discarded.

The PDs of a transformer typically display a much lower characteristic frequency than the PDs in a joint but their amplitude is higher. This is why PDs generated by the base-mounted transformer could be detected from quite some distance away. As illustrated in Fig. 7, the characteristic frequency of the PD observed at the base-mounted transformer was 30 MHz. At PA1555, located 337 m away, the characteristic frequency decreases to 7 MHz. As this frequency was picked up very efficiently by the earlier commercial device used, manhole access was prohibited for safety reasons when we reached the proximity of the TSS. The measurements taken with the PDA allowed us to lift the access restrictions.

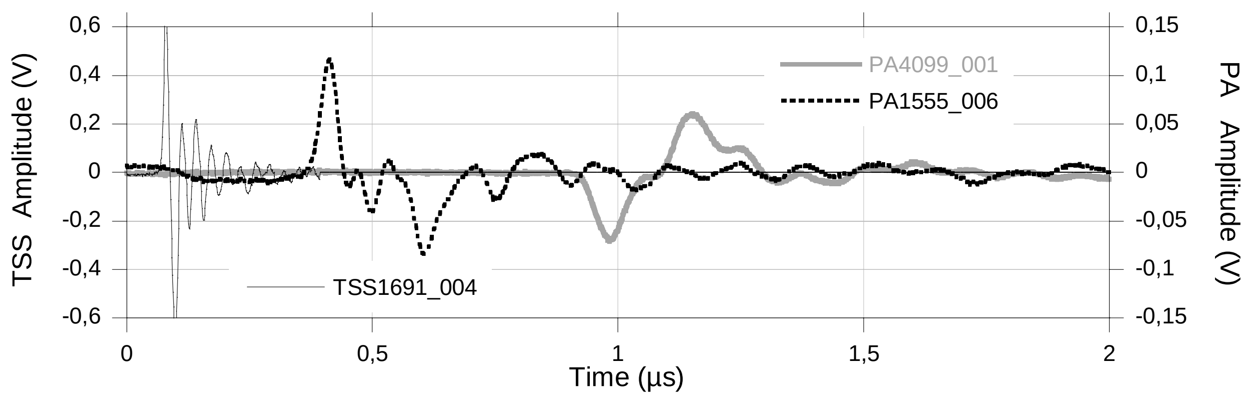

Figure 7: Discharges in a base-mounted transformer (TSS) observed in two manholes, PA1555 and PA4099, located 337 m and 609 m respectively from the transformer.

CONCLUSION

The partial-discharge analyzer developed in the course of this project has improved preventive maintenance and fulfils the strict requirements to guarantee safety for workers of the underground network. Despite the presence of considerable EM noise, the device is a highly reliable means of locating faults emitting partial discharges and confirming that equipment is free from PDs. The success obtained so far can be attributed to the highly detailed design, in particular the concept of time domain reflectometry using two wideband sensors, switchable analog and digital filters, time-frequency processing and the correlation of a number diagnostic explanations before selecting the most probable one. We owe this success also to our unlimited access to the system, the many withdrawals of equipment from the system in order to confirm the diagnostic and, lastly, our multidisciplinary approach.

ACKNOWLEDGMENTS

The authors thank fellow team members Yvan Roy, Sylvain Poirier, Richard L'Écuyer, Josée Caron, Jimmy Fournier, Jacques Bherer, René Morin and Michel Bissonnette for their indispensable contribution to this study. Thanks also go to the crews of splicers, technicians and thermographers who helped us with the on-line mesurements.

REFERENCES

[1] A. Gonzalez, 1990, *Portable device for the detection of partial discharges in energized cables and/or systems*, Canadian patent 2 013 552.

[2] D. Fournier & al., 2005, *Detection, location and interpretation of partial discharges in the underground network at Hydro-Québec*, Acts of the CIRED Conference, Turin.

[3] G. P. Van der Wijk et al., 1998, *Development and qualification of a new 400 kV XPLE cable system with integrated sensors for diagnostics*, CIGRE 1998, Paris, paper 21-103.

[4] E. F. Steennis, 1998, *Method and apparatus for measuring partial discharges in cables*, US Patent 5,767,684.

[5] D. Fournier, N. Amyot, 2001, *Diagnostic de l'échauffement excessif des raccords de câble dans le réseau souterrain*, Acts of the CIRED Conference, Amsterdam, Netherlands.

[6] T. Seghir et al., 2004, *The effect of temperature and the mutual influence between two cavities on the appearance of partial discharges in gaseous cavities contained in the insulator of high voltage,* ICSD 2004. vol.2, P.598-602.